Magnetotransport studies of the insulating phase around $\nu=\frac{1}{5}$ Landau-level filling

H. W. Jiang
MIT, Francis Bitter National Magnet Laboratory, Cambridge, Massachusetts 02139
and Princeton University, Princeton, New Jersey 08544

H. L. Stormer
AT&T Bell Laboratories, Murray Hill, New Jersey 07974

D. C. Tsui
Princeton University, Princeton, New Jersey 08544

L. N. Pfeiffer and K. W. West
AT&T Bell Laboratories, Murray Hill, New Jersey 07974
(Received 24 April 1991)

This paper presents a sequence of studies on electronic transport in high-mobility, two-dimensional electron systems in GaAs/$Al_xGa_{1-x}As$ heterostructures in high magnetic fields at low Landau-level filling factors where the formation of an electron solid has been postulated. It is an extension of our earlier work, summarizes our findings, and compares these findings with the results of other investigations. We observe a thermally activated insulating phase that surrounds the $\nu=\frac{1}{5}$ quantum liquid. This reentrant behavior is now documented for several samples of varying electron density and mobility. This broad universality of the phenomenon suggests an intrinsic mechanism as the cause for the transport features such as electron-solid formation, rather than individual carrier freeze out. Current-voltage measurements in the insulating phase reveal several anomalies. In low-voltage measurements we find nonlinearities similar to earlier results. An analysis of these data, which have been taken as convincing evidence for electron-solid formation, reveals some inconsistencies in the adopted model of charge-density depinning. In high-voltage measurements we observe the strong threshold behavior that also has been attributed, by yet more reports, to depinning of an electron solid. In our analysis we find a strong resemblance of this high-voltage breakdown to the breakdown behavior in the integer quantum Hall regime caused by a temperature runaway. Such a breakdown does not require a many-particle explanation. On the basis of our results, their analysis, and an assessment of the data in the literature, we believe that at the present time, in spite of some circumstantial evidence, there does not exist an experimental study that can positively identify the sought-after electron solid.

I. INTRODUCTION

The magnetic-field-induced Wigner solid in a two-dimensional electron system (2DES) has an unsteady history. Ever since the prediction of Lozovik and Yudson[1] in 1975 as to the formation of such a high-field electronic phase, there have been numerous reports on the supposed exposure of one of its characteristic signatures. In this way, many anomalies discovered in high-field magneto transport[2,3] and cyclotron resonance[4] of early experiments on Si-metal-oxide-semiconductor field-effect transistors were tentatively linked to the existence of an electron solid. The electron solids properties had meanwhile been further scrutinized in several theoretical papers.[5–9] With the advent of high-mobility 2DES in GaAs (Ref. 10) and the subsequent discovery of the fractional quantum Hall effect (FQHE),[11] the conditions for electron-solid formation needed to be revised. Since the multiple quantum fluids of the FQHE covered most of the extreme quantum limit,[12] an electron solid could only be expected in the small filling factor regime.

Early estimates by Laughlin of the FQHE–electron-solid transition[12] arrived at a value of $\nu_c\sim\frac{1}{10}$. With further theoretical work[13–17] on electron correlation at low filling factor, this value has now settled at $\nu_c\sim\frac{1}{6}$. Therefore a weak inflection in the derivative of the magnetoresistance around $\nu=\frac{1}{5}$ and its absence at $\nu=\frac{1}{7}$ observed by Mendez *et al.*[18] was then taken as evidence for the validity of this prediction. With the subsequent discovery of FQHE-like transport features at $\nu=\frac{1}{7}$ by Goldman, Shayegan, and Tsui,[19] such a simple view could no longer be upheld. However, experiments in the low-filling-factor regime by Willett *et al.*[20] found a curious thermal activation of the transport parameters at filling factors $\nu\lesssim\frac{1}{4}$. Although the data were not inconsistent with the formation of an electron solid, these experiments could not unambiguously identify the sought-after condensed phase.

Andrei *et al.*[21] reported detection of the characteristic $k^{3/2}$ dispersion of the lower magnetohybrid mode of the 2D electron solid by employing a radio-frequency technique. It was noticed[22] that a linear relationship between ω and k, uncharacteristic of any mode in such a solid, provided a superior fit to the data. This has invalidated the association of the radio-frequency response with the shear mode of the solid.

The nature of the electron state at exactly $\nu=\frac{1}{5}$ remained enigmatic to this point. There had been several reports[18–21,23–24] of local minima in the diagonal resistance R_{xx} at $\nu=\frac{1}{5}$. However, these features conspicuously disappeared on cooling to the lowest temperatures, vanishing into a steeply rising background. It remained uncertain whether the FQHE formed the true ground state at $\nu=\frac{1}{5}$ or whether some other phase, possibly the Wigner solid, prevailed at $T\rightarrow 0$, whereas a FQHE-like state existed at higher temperatures. This problem has now been resolved by Jiang *et al.*,[25] who observed vanishing resistance R_{xx} as $T\rightarrow 0$. This demonstrates that in low-disorder 2DES the FQHE prevails at $\nu=\frac{1}{5}$. Yet for $\nu<\frac{1}{5}$ and in a narrow region above $\nu=\frac{1}{5}$ the curious thermally activated transport behavior persists in contrast to the T dependence at any higher ν (lower magnetic field). If the earlier conjecture applies and exponential divergencies are indeed indicative of a pinned solid phase, then this solid must be reentrant around the $\nu=\frac{1}{5}$ FQHE. However, it is well understood that eventually the positive identification of the solid phase requires tools beyond the low-electric-field transport data, and even nonlinear I-V characteristics intended to induce depinning of the electron solid remain subject to a variety of interpretations. Experiments by Goldman *et al.*[26] and, more recently, Williams *et al.*[27] claim to have detected such an abrupt electric-field-induced depinning of the electron solid from residual impurity sites. Both groups use their data to promote an electron-solid–liquid phase diagram whose filling-factor dependence, incidentally, coincides with the regime of exponentially diverging R_{xx} seen in earlier transport data.[20]

The question of electron solid formation is now also addressed by magneto-optical experiments. A luminescence line apparent in magnetoluminescence data by Buhmann *et al.*[28] at filling factors $\nu<0.28$ is *ad hoc* attributed to the Wigner solid. The fact that its intensity decreases sharply around $\nu=\frac{1}{5}$, $\frac{1}{7}$, and $\frac{1}{9}$ is taken as evidence for further reappearances of quantum fluids at these filling factors. Recent measurements of the dynamical conductivity at small filling factors by surface acoustic waves[29] are interpreted as a pinning mode of the 2DES, which has condensed into an ordered phase.

In spite of all the past and recently increasing activities, we still lack the decisive experimental evidence for the existence of such a highly correlated electronic state. Only the unambiguous detection of a unique electronic mode and its linkage to a concrete excitation of the electron solid or the direct observation of the periodic arrangement of the electronic charges will eventually be able to establish the electron-solid phase. Even within the framework of the presently promoted circumstantial evidence for Wigner solid formation, there exist apparent inconsistencies among the data from different groups and considerable variations among supposedly characteristic parameters of the solid as determined by different techniques. For example, from the temperature-dependent disappearance of the conduction threshold both Goldman *et al.*[26] and Williams *et al.*[27] have derived phase diagrams. The relevant threshold voltages, however, differ by more than two orders of magnitude although similar magnetic fields are employed. The identified melting temperatures are roughly comparable in both experiments, lying mostly below 100 mK, whereas Buhmann *et al.*[28] assert to observe the solid by optical techniques clearly above 400 mK and probably at still higher temperatures.

Under such circumstances, it appears opportune to revisit the magnetotransport experiments, investigate different samples of varying electron density and mobility, and put the data in perspective to the published results. Like earlier studies, our findings cannot unambiguously identify the Wigner solid, however, they are able to shed some light on some of the unresolved issues and suggest some caution as to the interpretation of the bulk of experimental data.

II. EXPERIMENTAL DETAILS

Our 2DES's are fabricated by molecular-beam epitaxy as modulation-doped GaAs-(AlGa)As single heterostructures. Altogether 11 samples cut from 4 different wafers (A–D) are investigated. From low-field Hall measurements their density n and their mobility μ are determined for *A*: $n=1.1\times10^{11}$ cm^{-2}, $\mu=8\times10^{6}$ cm^2/V sec; *B*: 7.8×10^{10} cm^{-2}, $\mu=6\times10^{6}$ cm^2/V sec; *C*: $n=6.8\times10^{10}$ cm^{-2}, $\mu=4.5\times10^{6}$ cm^2/V sec; and *D*: $n=5.3\times10^{10}$ cm^{-2}, $\mu=2\times10^{6}$ cm^2/V sec. These densities and the exceedingly high mobilities are achieved after a short illumination with the red light from a light-emitting diode at about 1 K. The samples are of square shape with typical dimensions of 3×3 mm.^{2} The contacts consist of eight symmetrically placed, diffused In dots. The appearance of higher-orders states at $\nu=\frac{5}{11}$ and $\frac{6}{11}$ in magnetotransport experiments attests to the high quality of the specimens.

For electrical measurements, the samples are immersed in the dilute phase of the ^{3}He-^{4}He mixture of a dilution refrigerator with a base temperature of $\sim$60 mK. The temperature is determined from the resistance of calibrated Dale 750-Ω resistors which are well heat sunk to the samples. The temperature is corrected by a known magnetoresistance factor. Depending on the density of the sample, we employ three different magnet systems with peak fields between 12 and 31 T to reach the low-filling factor regime.

Electrical transport measurements are performed using standard, low-frequency lock-in techniques. Any such measurement in the low-filling factor regime is affected by the actual current distribution in the specimen. In particular, when operating in the vicinity of a conductor-insulator transition, minute inhomogeneities in carrier concentration may lead to considerable inhomogeneities in the current path. Ultimately, one has no exact knowledge of this distribution and cannot infer the homogeneity, or the lack of it, from electrical measurements along the perimeter of the sample. Eventually, any such measurement (ours, as well as those published in the literature; four-probe configurations as well as two-probe configurations) requires the assumption that the measured transport parameter reflect a bulk property. Since in the high-resistance regime, some contacts are found to

be rectifying at very small current levels, making them problematic as voltage probes, we have worked with both contact configurations. At low resistivities, $\rho_{xx} \lesssim \rho_{xy}$, where contacts are well behaved, we employ a four-probe contact configuration which measures the diagonal resistance $R_{xx} = \alpha \rho_{xx}$ ($\alpha \sim 1$ for our specimens). At high resistivities, $\rho_{xx} \gg \rho_{xy}$, we revert to a two-probe configuration which eliminates distortions due to voltage-probe nonlinearities. The contact resistance R_c is determined by monitoring the two-probe resistance at exactly $\nu = \frac{1}{5}$, which is the sum of the quantized Hall resistance $R_{xy} = 5h/e^2$ and R_c. In this way we are able to select contacts with negligible R_c in the relevant filling factor regime. Furthermore, since in the insulating phase the sample resistance can give rise to values as high as 10^8 Ω at temperatures below 100 mK, caution has to be exercised in selecting the excitation frequency to reduce the possible admixture of signals due to a stray capacitance of about 2 nF. A low frequency excitation of 4 Hz excludes such admixtures.

The current-voltage characteristics in the low-filling factor regime are determined by measuring either dV/dI or dI/dV in the voltage or current mode of a SR530 lock-in amplifier. A small ac modulation voltage or current is applied to the sample while a dc bias is swept.

III. RESULTS

A. Activated transport in the low-filling factor regime

Previously[25] we have shown that in the high-magnetic-field low-disorder limit, the ground state at $\nu = \frac{1}{5}$ Landau-level filling is an incompressible quantum liquid. This has been determined from the vanishing of R_{xx} as temperature approaches $T = 0$. Furthermore, at filling factors below $\nu = \frac{1}{5}$ (higher B field) as well as in a narrow region *above* $\nu = \frac{1}{5}$ (lower B field), R_{xx} diverges exponentially as $T \to 0$. We conclude that the FQH liquid at $\nu = \frac{1}{5}$ is surrounded by an insulating phase which may reflect the pinned electron solid. The concept of reentrance of the solid phase around a FQH liquid has now been further expanded in an *ad hoc* interpretation of optical data[28] to $\nu = \frac{1}{7}$ and $\frac{1}{9}$.

In this section we present further transport data in the vicinity of $\nu = \frac{1}{5}$ from a set of samples with different densities and mobilities. Within this range of transport parameters, we find qualitatively the same results as in our earlier publication. This demonstrates that reentrance of the insulating phase around the $\nu = \frac{1}{5}$ FQH liquid appears in a broad range of parameter space and is not limited to one specific specimen. In our transport measurement, whenever we were able to cover the filling factors $\nu = \frac{1}{7}$ and $\frac{1}{9}$ we invariably observed weak R_{xx} features at $\nu = \frac{1}{7}$ but not at $\nu = \frac{1}{9}$. However, in all cases the $\nu = \frac{1}{7}$ features disappeared riding on a rapidly rising background when cooling the sample to the lowest temperatures. It remains to be seen whether residual disorder destroys the energy gap at $\nu = \frac{1}{7}$ and $\frac{1}{9}$ or whether transport and optical measurements are sensitive to different aspects of the condensate.

Figure 1 shows an overview of a typical longitudinal resistance R_{xx} versus magnetic field at 100 mK. The high quality of the sample is reflected in the large number of higher-order FQHE states shown in the inset on an expanded scale. The large peak between $2/9 < \nu < 1/5$ stands out and grows exponentially on lowering the temperature. We identify this region as the first insulating phase which is followed by the neighboring $\nu = \frac{1}{5}$ quantum liquid indicated by its zero-resistance state. For $\nu < 1/5$, R_{xx} rises again dramatically with an exponential temperature dependence. This region is referred to as the second insulating phase.

Figure 2 shows the longitudinal resistance R_{xx} in an Arrhenius plot at $\nu = 0.21$ within the first insulating phase and at $\nu = 0.176$ within the second insulating phase. We observe clear activated behavior [$\propto \exp(E_a/2kT)$]. For one of the specimens from wafer D we determine R_{xx} at $\nu = 0.18$ from $0.12 < T < 1.0$ K (not shown) and confirm purely activated dependence without any indication of a phase transition over such an extended temperature range. In this case the resistance at high temperatures saturates to the magnetoresistance background and at low temperatures is limited to the maximum resistance ($\sim 10^9$ Ω) we can measure with any confidence.

Figure 3 shows the activation energy E_a as a function of filling factor around $\nu = \frac{1}{5}$ for three samples whose densities and mobilities vary significantly. In spite of this large variation in sample parameters and therefore magnetic fields, the filling factor dependences of the data appear remarkably similar. The activation energy increases rapidly from $\nu \sim 0.22$ to a peak at $\nu \sim 0.21$ and drops sharply towards the $\nu = \frac{1}{5}$ FQH liquid at $\nu = \frac{1}{5}$. For $\nu < 1/5$, E_a reappears, rises sharply to values higher than those at $\nu \sim 0.21$, and seems to saturate, at least in the two higher-density samples, towards lower filling factors. As to the absolute value of the activation energies, it is important to note that thermal cycling to room temperature can alter E_a within a given sample by as much as a factor of 2. However, during each low-temperature run all data are reproducible. The run-to-run variation mere-

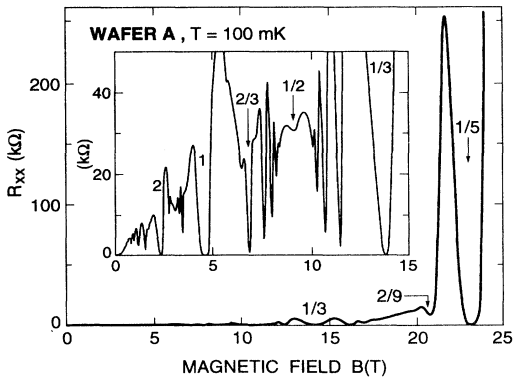

FIG. 1. Diagonal resistance R_{xx} vs magnetic field of sample from wafer A at $T = 100$ mK showing insulating phases surrounding $\nu = \frac{1}{5}$ quantum liquid. Inset shows on an expanded scale the low-field regime with many higher-order FQHE states.

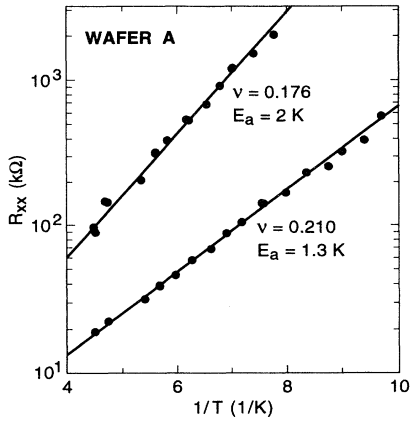

FIG. 2. Arrhenius plot of resistance in the first ($\nu=0.210$) and second ($\nu=0.176$) insulating phase of sample shown in Fig. 1. E_a is defined via $R_{xx} \propto \exp(E_a/2kT)$.

ly amounts to a variation of the vertical scales in Fig. 3.

Compared to the earlier data taken in this range of filling factor in Ref. 20, the activation energy shows much stronger variations. This is largely due to the reentrance of the insulating phase around the $\frac{1}{5}$ FQH liquid which causes the deep incision around the zero-resistance state of the liquid. The lack of this strong feature in the earlier data must be attributed to a higher level of disorder (supported by a somewhat lower mobility value) which destroys the quantum liquid gap. The slight depressions in E_a around $\nu=\frac{1}{5}$ in the earlier data are probably the remnants of the much stronger features seen in Fig. 3. Further comparison of our present results with the initial data indicates that the critical filling factors for onset of the activated longitudinal resistance around $\nu\sim0.22$ reproduce very well. In fact, the trend in critical filling factor versus B^{-1} (summarized in Ref. 20) showing the convergence towards $\nu\sim0.2$ for $B\rightarrow\infty$, continues quite satisfactorily (see Fig. 4) to include the data shown in Fig. 3. The general scale of activation energies ranging from $E_a\sim0.6$ K for the low-density sample to $E_a\sim2.0$ K for the high-density sample is comparable to the activation energies found at similar filling factors in Ref. 20. The tendency that higher-density samples have larger E_a at the low end of the filling factor scale is also reproduced, although the run-to-run variations in E_a for the data in Fig. 3 renders such a statement somewhat uncertain.

The saturation of the activation energy at low-filling factors, shown in the top panel of Fig. 3, is at variance with our earlier data[20] that showed a roughly linearly rising E_a with decreasing ν. However, again there is a clear trend from the low-density specimen (5.3×10^{10} cm^{-2}, which is comparable to the 4.5×10^{10} cm^{-2} sample of Ref. 20) to the high-density specimen (1.1×10^{11} cm^{-2}). With increasing density, the dependence of E_a on ν below $\nu\sim\frac{1}{5}$ appears to flatten successively reaching a clearly saturated behavior at the highest carrier concentration. In summary we can trace a continuous evolution of the characteristic shape of E_a vs ν as the electron density n and/or electron mobility μ increases. In our high-mobility samples n and μ typically vary together and it is, therefore, not possible to clearly separate mobility dependences from density dependences.

We believe that the data of Fig. 3 provide further evidence that the insulating regions around $\nu=\frac{1}{5}$ are caused by an intrinsic electronic phase, such as the pinned electron solid, rather than individual carrier freezeout. We have argued before[25] that the exponential increase in R_{xx}

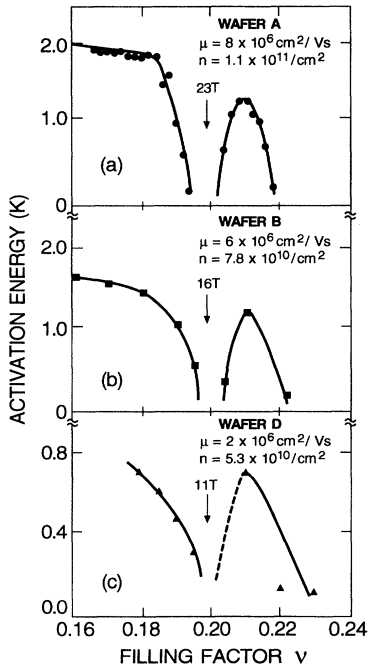

FIG. 3. Activation energy vs filling factor for three samples. In spite of a significant difference in mobilities and densities the general shape of the curves is very similar.

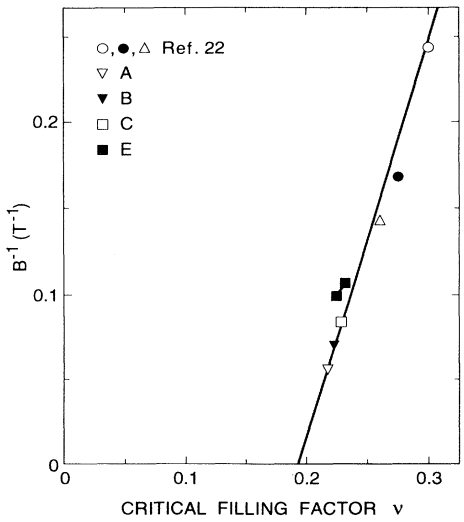

FIG. 4. Critical filling factor ν_c for onset of exponential temperature dependence vs inverse magnetic field at onset using $B^{-1}=e\nu/nh$. The critical filling factor extrapolates towards $\nu\approx0.2$ for $B\rightarrow\infty$.

with decreasing T is unlikely from single-particle localization due to disorder. The disorder in a sample, which is not sufficiently strong to localize electrons at $\nu=\frac{1}{5}$, is not likely to cause electron localization at *lower B*. The same behavior with similar characteristics seen over a broad range of transport parameters in Fig. 3 supports this earlier conjecture. Numerical calculations in this filling factor regime indicate a close proximity in the ground-state energies between the electron solid and the quantum liquids.[14,17] Furthermore, a close inspection[25] of the energetics in the vicinity of $\nu=\frac{1}{5}$ provides a sound rationale for the reentrance of the solid phase around the $\frac{1}{5}$ FQH liquid. The totality of these observations, therefore, strengthens our earlier proposal.

Within such a model of electron-solid formation the transport characteristics arise from pinning the solid to residual disorder sites.[30] A pinned electron solid is then expected to be an insulator. An analogy can be drawn to the conduction of pinned charge-density waves (CDW's) in materials such as $NbSe_3$.[31]

In the 2D electron solid all electrons are expected to be pinned at low temperatures. The finite conductivity at finite temperatures may then be caused by activation of electrically charged defects.[20] Chui and Esfarjani[32] have recently proposed a model of thermally activated dislocation created within the solid as the carriers of electronic charge at finite temperatures. Their model further can account for the roughly linear dependence of E_a vs ν observed in earlier data and their calculated values for E_a agree roughly with those of the experiments. The results on the high-mobility specimens seen in Fig. 3 indicate a somewhat more complex filling factor dependence of the activation energy than originally assumed. Although the general energy scale for the Chui and Esfarjani mechanism continues to fall within the experimental results, further refinements of such a model are required to account for the experimental trends.

B. Current-voltage characteristics

1. Small-voltage limit ($V \lesssim 1$ mV)

As observed by Willett *et al.*,[33] and more recently by Goldman *et al.*,[26] the current-voltage characteristic in the region of activated R_{xx} behavior is nonlinear. While Ref. 33 was alluding to the possibility of electric-field-induced depinning of the electron solid, it provided also an alternative interpretation in terms of inhomogeneous transport in the 2D plane and electric breakdown across current carrying filaments. Goldman *et al.*[26] interpret their data in terms of electron-solid depinning and derive a definite solid-liquid phase diagram from their results.

We have reinvestigated the I-V characteristics in our high-mobility, high-density samples and make the following observations.

(i) At low temperatures we observed, similar to earlier reports,[26,33] a threshold field E_c at which the low-field, Ohmic conduction changes to a high-field, non-Ohmic conduction as seen in Fig. 5(a). (For our sample dimensions $E_c \approx 3\ \mathrm{cm}^{-1} V_c$.)

(ii) Raising T causes E_c to vanish and smears out the transition as seen in Fig. 5(b).

(iii) The temperature T_c at which the threshold field appears to have vanished varies from cooldown to cooldown by as much as a factor of 2.

The current interpretation of these features in the I-V characteristic presumes a depinning of the 2D electron solid or CDW: At vanishing electric field the electron solid is pinned to random disorder sites and there is no contribution to the conduction from the pinned solid. Its residual finite conductivity is from thermally activated charged dislocations of the solid as described in Sec. III A. When a critical electric field E_c has been reached, the solid breaks loose from its pinning sites and its sliding motion adds to the electrical conduction.[30,31,34,35] As the temperature is raised, the electron solid melts and the associated temperature establishes the critical solid-liquid transition temperature at this specific Landau level filling factor ν.

Although this model represents a very attractive scenario for the interpretation of the experimental results, it also has inconsistencies: One would expect a sudden depinning of the solid to cause a sharp break in the I-V and, hence, a *step* in the differential resistance of Fig. 5. Such steps have indeed been observed in lower-mobility samples,[33] but are absent in the more recent data. The interpretation of data such as Fig. 5 requires then either a nonlinear resistance of the sliding charge density or a very broad distribution of pinning energies, with E_c being the threshold for the weakest of the pinned domains. The non-Ohmic conduction beyond E_c is

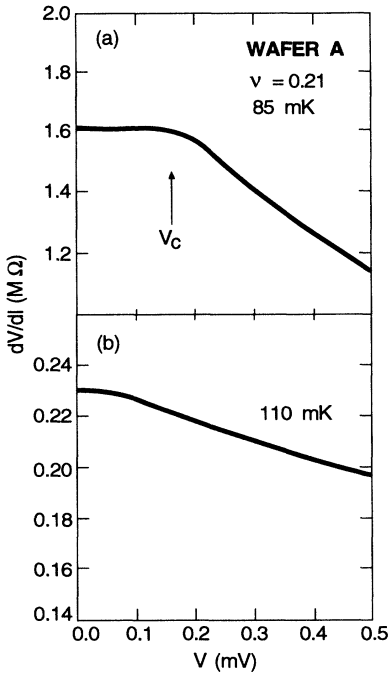

FIG. 5. Differential resistance (dV/dI) vs applied voltage (V) within the first insulating phase at a fixed filling factor of $\nu=0.21$ for two different temperatures. The sample has the shape of a 3×3 mm^2 square. In trace b the critical voltage V_c has shrunk to $V_c \sim 0$.

caused by the successive depinning of domains with increasingly higher pinning energies. In both interpretations the nonlinear regime of the I-V characteristics necessitates the existence of a solid phase beyond E_c. Therefore the most disturbing aspect of the proposed model of depinning of an electron solid is the deduction of a solid-liquid phase diagram from data such as Fig. 5. The melting temperature $T_m(\nu)$ is equated with the temperature at which, for each filling factor ν, the critical field E_c vanishes, such as seen in Fig. 5(b). However, the non-Ohmic behavior remains and it persists in our experiments up to temperatures that exceed the so-determined melting temperature T_m by more than a factor of 2 to 3 . This leads to the contradiction between the transition to a liquid due to a vanishing threshold voltage and the existence of a solid due to persisting non-Ohmic characteristics. Furthermore, in a typical CDW material the depinning field E_c diverges as T approaches T_m.[36,37] This feature is absent in our data and the data of Ref. 26. A correlation between the temperature T_m of vanishing threshold voltage and the appearance of excessive broadband noise below T_m has been taken as further evidence for the melting of a postulated electron solid.[26] Curiously the voltage threshold for this signal exceeds the threshold for non-Ohmic conduction by more than an order of magnitude. While the appearance of excessive noise is a necessary consequence of the sliding motion, it is by no means sufficient for the implication of an electron solid. Other breakdown phenomena, such as impact ionization of localized carriers, will generate similar noise enhancement. It is *narrow*-band noise that provides firm evidence for the existence of an underlying charge modulation such as in a CDW or an electron solid. This signature of the electron solid remains unobserved.

The conflicts within the model for the interpretation of the I-V characteristics are also evident in the temperature dependence of R_{xx} for different measuring voltages. Figure 6 shows as an example of three Arrhenius plots of R_{xx} at $\nu=0.185$ for sample D measured using three different voltages $V=0.1$, 4 and 10 mV. In this sample the threshold voltage is about 0.2 mV. In spite of the broad range of voltages from below the threshold voltage to high above the threshold voltage, there is no qualitative difference in the activated transport behavior. In the low-voltage data, taken in the Ohmic regime, there is no signature at the supposed solid-liquid transition temperature of $T_c \sim 120$ mK as deduced from vanishing E_c. Furthermore, the activation energies derived from Fig. 6 are very similar and independent of the electric field. They are insensitive to whether the electron solid is pinned or sliding.

In summary, it appears that the interpretation of nonlinear transport at low-Landau-level filling factors in terms of the depinning of an electron solid and a melting of this phase at higher temperatures remains inconclusive and further critical examination of the data is called for.

2. *High-voltage limit ($V \gg 1$ mV)*

Whereas most of the investigations on nonlinearities in the I-V characteristics have focused on the low-voltage regime, Williams *et al.*[27] have reported giant nonlinearities at 100 to 1000 times higher voltages. Following their protocol they assign the features to depinning of the electron solid and derive another phase diagram. The sample size and the 2DES parameters are rather similar to those of Refs. 26 and 33, although the onset voltages for the nonlinear conduction is a factor of 10^2 to 10^3 larger. Such large ranges in the breakdown voltages are difficult to consolidate. Although a theoretical model that allows for more than one depinning field has just been proposed,[38], it remains uncertain whether the experimental data can be interpreted in this way.

We have also investigated this high-voltage regime in our samples. Indeed all our specimens show the high-voltage breakdown in *addition* to the low-voltage nonlinearities described in Sec. III B 1. Figure 7 presents a set of experimental traces of dI/dV taken at different filling factors ν at 82 mK as a function of voltage. These measurements were performed in a two-probe configuration which limits the conductance to $\nu e^2/h \sim 6-7\times10^{-6}\ \Omega^{-1}$ in the high-voltage limit for the filling factor range of Fig. 6. The distance between the contacts is about $\frac{1}{3}$ cm. These traces clearly demonstrate very low conductance levels below some threshold field at which a sharp transient occurs, followed by a reduction to a level of $\nu e^2/h$ limited by the two-terminal geometry.

These breakdown features in dI/dV are very similar to those observed by Williams *et al.*[27] and are observed in the same parameter space. These authors identify the sharp onset of conductivity as the threshold for depinning of the electron solid and derive from it a solid-to-liquid phase diagram. In our case, such an identification would be incorrect and the transport in the voltage region below the transient is non-Ohmic consistent with the data of Refs. 26 and 33. To enhance the sensitivity to low-level conductances, we show in Fig. 8 a representative of the data from Fig. 7 on a semilogarithmic scale. The conductance below threshold is by no means Ohmic but increases exponentially by as much as a factor of 20 between $V\sim0$ and the threshold voltage. This observation cannot be directly related to a simple depinning of an electron solid. To investigate further these features at high voltages, we plot in Fig. 9 the threshold voltage as well as the power dissipation at the threshold versus

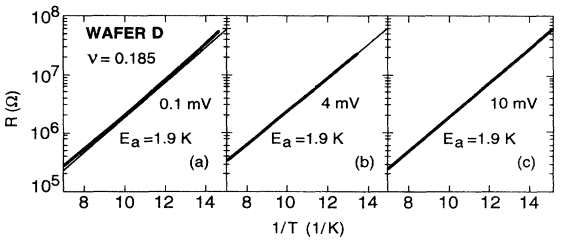

FIG. 6. Arrhenius plots of two-terminal resistance R in the second insulating phase of wafer D at fixed filling factor $\nu=0.185$. R is measured differentially as $(dI/dV)^{-1}$. The heavy line is the data taken quasicontinuously. The activation energy E_a is practically independent of drive voltages, although their values span from below the critical voltage $V_c=0.2$ mV to far above it.

filling factor. Despite the fact that the threshold voltage varies considerably with filling factor, the power dissipation stays practically constant at 0.2 nW. This phenomenon bears a surprisingly strong resemblance to the non-Ohmic conduction found earlier in the regime of the integral quantum Hall effect[39–41] which was explained by Komiyama *et al.* as the consequence of electron heating. The electrons dissipate their energy to the GaAs crystal through electron-phonon coupling. For increasing power input, the electron temperature T_e exceeds the lattice temperature T_l. Since the conductivity σ_{xx} is strongly temperature dependent, there eventually develops an instability at which the electronic transport undergoes a transition to a high-current carrying state. These conditions are very similar to the conditions for transport in the low-filling factor regime examined here.

The model of Komiyama *et al.* is based on a balance equation between power input into the electron system $P=\sigma_{xx}E^2$ and power losses to the GaAs host $[\Xi(T_e)-\Xi(T_l)]/\tau_\varepsilon=P$. $\Xi(T)$ is the energy per unit area of the electron system at temperature T and τ_ε is the energy relaxation time. With the simple assumptions that $\Xi(T)$ is the product of the Landau-level density of states times the Fermi distribution at T and that τ_ε solely depends on T_e, Komiyama *et al.* achieve a quantitative description of the experimental data for the breakdown in the IQHE. We did not attempt to develop an equivalent quantitative model for the breakdown observed in Ref. 27 and seen in Fig. 6. However, with the reasonable assumption that the Landau-level density of states and, therefore, $\Xi(T_e)$ is not explicitly dependent on ν for the small range of Fig. 7, the breakdown power P_c derived from the above balance equation becomes independent of ν. This is the behavior we observe and show in Fig. 9. The independence of the breakdown power from the filling factor is, therefore, consistent with a simple interpretation of the high-field breakdown as being caused by excessive electron heating. Such a simple model for the high-field threshold behavior should, therefore, not be ignored.

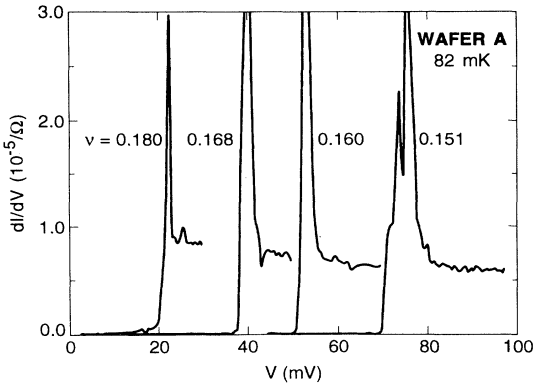

FIG. 7. Differential conductance (dI/dV) vs drive voltage in sample from wafer A. The data are taken at fixed temperature and at four different filling factors in the second insulating phase.

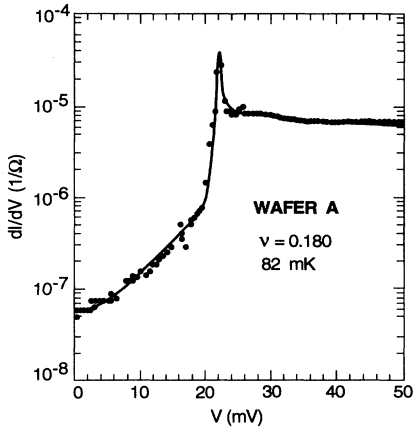

FIG. 8. Differential conductance of Fig. 7 on semilogarithmic scale. The conductance varies by as much as a factor of 20 below the breakdown voltage.

IV. SUMMARY

In this paper we present a more comprehensive study of electronic transport in high-mobility two-dimensional systems in the low-filling factor regime around $\nu=\frac{1}{5}$. In low-voltage, temperature-dependent transport we find an insulating phase surrounding the $\nu=\frac{1}{5}$ quantum liquid as $T\rightarrow 0$. For finite temperature the transport of this phase is thermally activated. Its activation energy $E_a(\nu)$ is filling factor dependent, has a threshold in the vicinity of $\nu\sim 0.22$, and extends toward $\nu\rightarrow 0$ interrupted only by the $\nu=\frac{1}{5}$ FQH liquid. While the detailed shape of E_a vs ν is density and mobility dependent, all data show the universal features of a common onset and a reentrance around $\nu=\frac{1}{5}$. There is also a general trend towards higher values of activation energies and a progressive saturation of $E_a(\nu\rightarrow 0)$ for higher density samples (which require higher magnetic fields.) The universality of this behavior suggests an intrinsic origin, such as a pinned solid phase rather than individual carrier freezeout.

Current-voltage characteristics reveal several additional features. At low voltages we observe a transition from

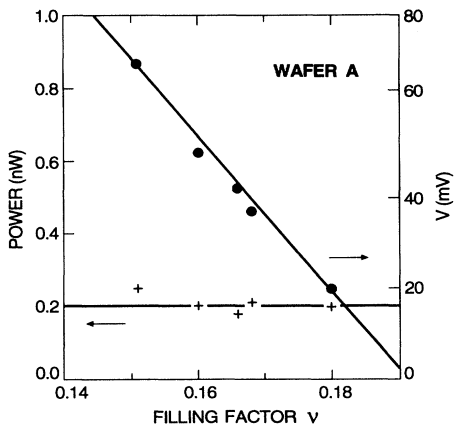

FIG. 9. Threshold voltage (circles) and input power at threshold (crosses) vs filling factor for data from Fig. 7.

Ohmic to non-Ohmic behavior which has earlier[26] been attributed to depinning of the solid phase. In our analysis, following such a model, we find apparent contradictions that we are unable to resolve. We, therefore, suggest that the direct association of the nonlinearities with depinning of the electron solid in this filling factor regime requires further experimental studies and a careful reexamination of the existing data. At voltages about 100 times higher, we observe dramatic breakdown behavior which also has been attributed to depinning of an electron solid in Ref. 27. We find that these high-voltage thresholds are reminiscent of breakdown phenomena in the IQHE which are caused by electron heating and subsequent thermal runaway. The interpretation of such data, therefore, does not require the existence of a pinned electron solid. Based on our analysis we believe that at the present time there does not yet exist an experimental study which can unambiguously identify the sought-after electron solid. Such a positive identification will require the observation of an electronic mode characteristic of the electron solid or the demonstration of a periodic arrangement of its constituents.

ACKNOWLEDGMENTS

We would like to thank Kirk Baldwin for excellent technical support, A. J. Dahm, P. B. Littlewood, and S. N. Coppersmith for helpful discussions, and the staff of the Francis Bitter National Magnet Laboratory for their hospitality. H. W. J. and D. C. T. are supported through the NSF Grant No. DNR-8919528.

[1]Y. E. Lozovik and V. I. Yudson Pis'ma Zh. Eksp. Teor. Fiz. **22**, 26 (1975) [JETP Lett. **22**, 11 (1975)].
[2]S. Kawaji and J. Wakabayeshi, Solid State Commun. **22**, 87 (1977).
[3]D. C. Tsui, Solid State Commun. **21**, 675 (1977).
[4]B. A. Wilson, S. J. Allen, Jr., and D. C. Tsui, Phys. Rev. Lett. **44**, 479 (1980).
[5]H. Fukuyama, Solid State Commun. **19**, 551 (1976); **17**, 1323 (1975).
[6]M. Tsukada, J. Phys. Soc. Jpn. **42**, 391 (1977).
[7]H. Fukuyama, P. M. Platzman, and P. W. Anderson, Surf. Sci. **73**, 374 (1978); Phys. Rev. B **19**, 5211 (1979).
[8]Y. Kuramoto, J. Phys. Soc. Jpn. **44**, 1035 (1978).
[9]H. Aoki, J. Phys. C **12**, 633 (1979).
[10]H. L. Stormer, R. Dingle, A. C. Gossard, W. Wiegmann, and M. D. Sturge, Solid State Commun. **29**, 705 (1979).
[11]D. C. Tsui, H. L. Stormer, and A. C. Gossard, Phys. Rev. Lett. **48**, 1559 (1982).
[12]R. B. Laughlin, Phys. Rev. Lett. **50**, 1395 (1983).
[13]K. Maki and X. Zotos Phys. Rev. B **28**, 4349 (1983).
[14]P. K. Lam and S. M. Girvin, Phys. Rev. B **30**, 473 (1984).
[15]D. Levesque, J. J. Weiss, and A. M. MacDonald, Phys. Rev. B **30**, 1056 (1984).
[16]S. T. Chui, T. M. Hakim, and K. B. Ma, Phys. Rev. B **33**, 7110 (1986).
[17]K. Esfarjani and S. T. Chui, Phys. Rev. B **42**, 10 758 (1990).
[18]E. E. Mendez, M. Heiblum, L. L. Chang, and L. Esaki, Phys. Rev. B **28**, 4886 (1983).
[19]V. J. Goldman, M. Shayegan, and D. C. Tsui, Phys. Rev. Lett. **61**, 881 (1988).
[20]R. L. Willett, H. L. Stormer, D. C. Tsui, L. N. Pfeiffer, K. W. West, and K. W. Baldwin, Phys. Rev. B **38**, 7881 (1988).
[21]E. Y. Andrei, G. Deville, D. C. Glattli, F. I. B. Williams, E. Paris, and B. Etienne, Phys. Rev. Lett. **60**, 2765 (1988).
[22]H. L. Stormer and R. L. Willett, Phys. Rev. Lett. **62**, 972 (1989).
[23]R. L. Willett, H. L. Stormer, D. C. Tsui, A. C. Gossard, J. H. English, and K. W. Baldwin, Surf. Sci. **196**, 257 (1988).
[24]J. R. Mallett, R. G. Clark, R. J. Nicholas, R. L. Willett, J. Harris, and C. T. Foxon, Phys. Rev. B **38**, 2200 (1988).
[25]H. W. Jiang, R. L. Willett, H. L. Stormer, D. C. Tsui, L. N. Pfeiffer, and K. W. West, Phys. Rev. Lett. **65**, 633 (1990).
[26]V. J. Goldman, M. Santos, M. Shayegan, and J. E. Cunningham, Phys. Rev. Lett. **65**, 2189 (1990).
[27]F. I. B. Williams, P. A. Wright, R. G. Clark, E. Y. Andrei, G. Devill, D. C. Glattli, O. Probst, B. Etienne, C. Dorin, C. T. Foxon, and J. J. Harris, Phys. Rev. Lett. **66**, 3285 (1991).
[28]H. Buhmann, W. Joss, K. von Klitzing, I. V. Kukushkin, A. S. Plaut, G. Martinez, K. Ploog, and V. B. Timofeev, Phys. Rev. Lett. **66**, 926 (1991).
[29]M. A. Paalanen, R. L. Willett, R. R. Ruel, K. W. West,, L. N. Pfeiffer, D. J. Bishop, and P. B. Littlewood (unpublished).
[30]H. W. Jiang and A. J. Dahm, Phys. Rev. Lett. **62**, 1396 (1989).
[31]N. P. Ong and P. Monceau, Phys. Rev. B **16**, 3443 (1977).
[32]S. T. Chui and K. Esfarjani, Phys. Rev. Lett. **66**, 652 (1991).
[33]R. L. Willett, H. L. Stormer, D. C. Tsui, L. N. Pfeiffer, K. W. West, M. Shayegan, M. Santos, and T. Sajoto, Phys. Rev. B **40**, 6432 (1989).
[34]H. Fukuyama and P. A. Lee, Phys. Rev. B **17**, 535 (1978).
[35]S. T. Chui, Phys. Rev. B **19**, 4333 (1979).
[36]P. A. Lee and T. M. Rice, Phys. Rev. B **19**, 3970 (1979).
[37]R. M. Fleming, Phys. Rev. B **22**, 5606 (1980).
[38]B. G. A. Normand, P. B. Littlewood, and A. J. Millis (unpublished).
[39]G. Ebert, K. von Klitzing, K. Ploog, and G. Weimann, J. Phys. C **16**, 5441 (1983).
[40]M. E. Cage, R. F. Dziuba, B. F. Field, E. R. Williams, S. M. Girvin, A. C. Gossard, D. C. Tsui, and R. J. Wagner, Phys. Rev. Lett. **51**, 1375 (1983).
[41]S. Komiyama, T. Takamash, S. Hiyamizu, and S. Sasa, Solid, State Commun. **54**, 479 (1985).